Atomic Force Microscopy and Experiments*

Kazem Ayat†
Physics Department, University Of California: Berkeley
(Dated: March 14, 2023)

Abstract

During our experimental work, we utilized a commercially available AFM unit and conducted five distinct experiments. Initially, we focused on acquiring a deep understanding of the AFM microscope and the various factors that influence its functioning. We carefully examined both internal and environmental sources of noise and how they impact the accuracy of the instrument. Following this, we shifted our focus to scanning optical disks and employed the AFM to accurately measure the pit depths of these disks, achieving a remarkable 20 percent accuracy rate. We also utilized the phase drive scan technique to analyze the structure of a polymer sample in detail, further refining our understanding of the AFM's capabilities. Finally, we delved into the F-D curve experiment and utilized it to estimate the Boltzmann constant with remarkable precision, achieving a difference of merely 1 percent from the accepted value. Through our efforts, we have gained a deeper appreciation for the versatile capabilities of AFM units and the significant contribution they can make to scientific research.

I. INTRODUCTION: WHAT IS AFM?

Atomic force microscopy (AFM) is a powerful imaging technique that allows the measurement of nanoscale features and properties of materials. It is a high-resolution scanning probe microscopy technique that uses a sharp tip to scan a sample surface to generate topographic images at the nanometer scale. The tip is mounted on a cantilever, which is deflected by the interactions between the tip and the sample surface. The deflection is measured by a laser beam that reflects off the back of the cantilever and onto a photodiode.

AFM was first introduced by Gerd Binnig, Calvin Quate, and Christoph Gerber in 1986, who was awarded the Nobel Prize in Physics for their invention in 1986. Since then, AFM has become a widely used technique in a variety of fields, including materials science, biology, physics, and chemistry.

AFM can provide information about the surface topography, roughness, and mechanical properties of materials. It can also be used to study surface chemistry and to image biological samples. The versatility of AFM arises from the fact that the interaction forces between the tip and the sample surface can be tailored to probe a wide range of physical and chemical properties.

The AFM easily can be considered the best way of microscopy in most cases. As a quick proof, it is worth introducing some other types of microscopy techniques. There are several types of microscopy techniques, including Scanning Tunneling Microscopy (STM), Transmission Electron Microscopy (TEM), Scanning Electron Microscopy (SEM), and Optical microscopy. STM scans the surface of a conductive sample to create an image with atomic resolution, TEM uses a beam of electrons to reveal the internal structure of a sample at high resolution, and SEM scans the surface of a sample to create a high-resolution 3D image of its surface morphology. Optical microscopy, on the other hand, uses visible light and lenses to magnify and view specimens.

The most common type of microscopy is indeed optical microscopy. This particular method is at a disadvantage compared with AFM. Since optical microscopy does not offer information regarding the height of the sample. It is merely a 3D top-view view of the sample of interest. While AFM provides detailed information in all 3 axes of position. AFM could be used to measure the height of surface features with high accuracy, making it useful for measuring the thickness of thin films or the dimensions of nano-structures. Note that the Optical microscopes could be used as a great complimentary tool with the AFMs for visual fine-tuning purposes such as tuning the probe's point on the desired location, etc. AFM can provide information about the stiffness, elasticity, and adhesion of materials. This makes AFM useful for studying the mechanical properties of biological tissues or for characterizing the mechanical properties of materials for applications such as microelectronics or nano-materials.

To address the limitations of the STM, the AFM was developed as a version of the scanning tunneling microscope that would be more capable of imaging biological samples. Despite the STM being considered a fundamental advancement for scientific research, it had limited applications since it could only work on electrically conductive samples. AFM has a great advantage in that almost any sample can be imaged, be it very hard, such

* From now on we call Atomic Force Microscopy as AFM
† Also at Physics Department, University Of California:Berkeley

as the surface of a ceramic material, or a dispersion of metallic nanoparticles, or very soft, such as highly flexible polymers, human cells, or individual molecules of DNA. There is minimal sample preparation required with an AFM, and nearly any sample can be measured. With an AFM, if the probe is good enough, a good image is measured. Because TEM and SEM usually operate in a vacuum and require a conductive sample (so non-conductive samples are usually coated with a metallic layer before imaging), AFM has the advantage of being able to image the sample with no prior treatment, in an ambient atmosphere. AFM's other key advantage is its very high sensitivity and the fact that the smaller the instrument, the more sensitive it can be. An AFM is rather different from other microscopes because it does not form an image by focusing light or electrons onto a surface, like an optical or electron microscope. An AFM physically literally 'feels' the sample's surface with a sharp probe, building up a map of the height of the sample's surface(a.k.a Spatial resolution).

Well, now AFM is simply the best tool for many microscopy purposes, but they come with a simple disadvantage, which is really negligible compared to all its great benefits. AFM is not practical to make measurements on areas greater than about 100 μm. This is because the AFM requires mechanically scanning the probe over a surface, and scanning such large areas would generally mean scanning very slowly. Exceptions to this include parallel AFM that measure small areas but with many probes to build up a large dataset, or "fast scanning' AFM's". AFM image recording is usually slower than an SEM, so if a large number of features on one sample are required, AFM may be considerably slower than SEM for the same sample. To conclude AFM is among the most useful and convenient laboratory tools, and techniques.
In This report, we are going to go over the use of an AFM system, and calibration of the system, the theory behind it and experiments, and how it works. We also cover the required editing techniques for an AFM image and 3D picture sample in Gwyddion editing software. Then do 5 series of experiments in which Atomic force microscopes plays a central role in. These experiments in order of increasing complexity are:

1. Noise Floor Experiment
2. CD/DVD Experiment
3. Polymer Glue Experiment
4. Force Distance Curve Experiment
5. Boltzmann's's Constant Experiment

Then provide the results of all experiments plus all the data analysis and required error analysis.

II. THEORY

In this section we will cover the working principles behind an AFM system AND Also will cover the theory behind those 5 promised experiments.

A. Principles Behind AFM

The major components in a regular AFM are but are not limited to a position-sensitive photo-detector, a laser, a mirror, and a tip. A cantilever. The cantilever is actually could be modeled as a spring with a certain spring constant "k" (fig.1). There is also a piezo material that works as a very key item in AFM which we call z-piezo from now on. Z-piezo can expand or contract around zero points based on the voltage applied! It is used to account for the changes in height of the needle, changes in the forces in the cantilever, and by moving the z-piezo so it can maintain the constant frequency and amplitude as before in the vibrating mode! This material enables us to scan the sample with high resolution! We always deal with piezo materials in our daily life! The lighter and stoves all use a piezo material to ignite the spark!

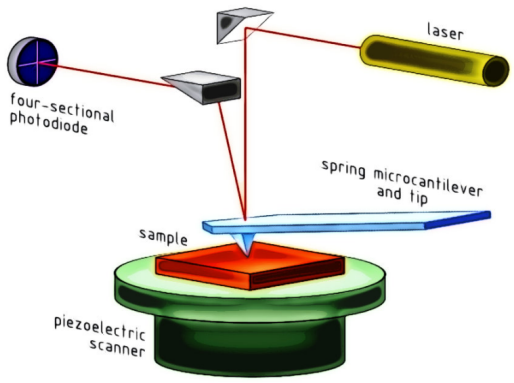

FIG. 1. The components and interiors of an AFM system.[2]

There are 2 Modes associated with the AFM machines.

1. Non-Vibrating mode (Non-Contact) (for Boltzmann constant and Force-distance curve Experiment)
   (a) Constant force
   (b) Constant height
2. Vibrating mode (contact) (rest of the lab)

The way that these modes works is on the basis of Columbs Force. Both vibrating and non-vibrating modes work similarly in spirit. Let us start with the non-vibrational mode. In this mode as indicated we also have two different modes: Constant force, and constant height!

In the constant force method, the goal is to keep the deflection (or the force F= - k D) constant (D for deflection). The changes in the deflection of the cantilever will be recorded by the change in the position of the laser in the position-sensitive photo-detector! Now, this mode benefits from a feedback loop. Once the position of the laser changes from the center point of the origin of the position-sensitive photo-detector, the Z-piezo will adjust its height by applying some voltage to account for this change of height, and once again the z-piezo is level and the laser is in fact at the origin of the position-sensitive photo-detector! So we can find the change in height by the change in z-piezo. Once more, note that this mode uses a feedback loop to apply some voltages to z- piezo and lift it up so the apparatus is level once again!

The other option within non-vibrational mode is constant height. This method will be performed operationally much faster but comes at the cost of less accuracy. Hence, we will not use this mode. But for the sake of completeness, we will discuss them here a bit. In this option, the z-piezo's height is kept constant and won't change. Then it should monitor how the cantilever deflects as it is scanning the surface and mapping out the deflections directly to topography maps.

The next mode is the Vibrational mode and will be used in the majority of the experiments (all experiments other than the Boltzman and Force-distance curve Experiments.). In this lab as it is hinting by the name we are driving the cantilever by a certain frequency. If the tip is far from the sample, the output signal will look like a regular Sin wave. However, as we approach the surface the frequency will increase and the cantilever will be damped and the frequency will be changed. This essentially works as the basis of the feedback loop in this mode. The system will try to keep the oscillations and the amplitudes at a constant frequency. According to the introduced feedback loop, once the system notices a difference in frequency and amplitude, it will respond by moving the z-piezo so it can maintain the constant frequency and amplitude as before! Hence monitoring the adjustments of the z-piezo gives us the height difference on the surface! So instead of the constant deflection (as in constant-force, non-vibrating mode), now the system tries to keep the frequency and amplitude constant. Basically, the ultimate goal of the AMF machines is to keep something constant. These modes come in useful in different applications and situations. Note that the special unit AFM workshop that we work with in this lab, is changing the location of the sample in the x-y plane instead of changing the needle tip in the x-y plane. But the z direction will be changed directly by the needle as promised.

Naturally as readers could guess, modeling the Cantilever as a spring helps us to understand the system so much better. Since the it is modeled as a spring, then the force will follow the Hook's law:

$$F = -kD$$

Where D is the deflection amount, and k is spring constant $k \equiv mw_0^2$.

B. Principles Behind Experiments

One of the most critical parts of this lab report is measuring Boltzmann's constant. This constant could be easily found using principles behind thermal physics and of course, modeling the cantilever's tip as a simple harmonic oscillator!
So then if we model the cantilever as a simple harmonic oscillator, we can say that the Hamiltonian will be of the form:

$$\mathcal{H} = \frac{p^2}{2m} + \frac{m\omega_0^2 z^2}{2}$$

By equipartion Theorem We know that the average value of each quadratic term in the Hamiltonian is given by $\frac{1}{2}K_BT$, hence:

$$< \frac{1}{2}mw_0^2z^2 >= \frac{1}{2}K_BT$$

$$< \frac{1}{2}kz^2 >= \frac{1}{2}K_BT$$

$$\frac{1}{2}k < z^2 >= \frac{1}{2}K_BT \tag{1}$$

where $k \equiv mw_0^2$. Note that $< z^2 >$ is actually the average of the cantilever's oscillations in the vertical direction.

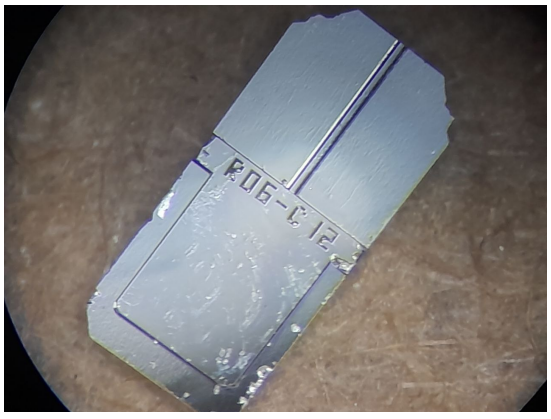

FIG. 2. A probe under an optical microscope. The cantilever is even smaller and can not be seen here!

C. Miscellaneous theory

Lagrange polynomial is a mathematical tool used in numerical analysis and interpolation to approximate a function using a polynomial of a specific degree.

The Lagrange polynomial is constructed by fitting a polynomial of degree n to a set of $n+1$ data points. The polynomial passes through each of the data points and is uniquely determined by them.

Given a set of $n+1$ data points (x_i, y_i), where $i = 0, 1, ..., n$, the Lagrange polynomial $L_n(x)$ of degree n is defined as:

$$L_n(x) = \sum_{i=0}^{n} y_i \prod_{j=0, j\neq i}^{n} \frac{x - x_j}{x_i - x_j}$$

The Lagrange polynomial $L_n(x)$ is a polynomial of degree n that passes through all $n+1$ data points (x_i, y_i). Each term in the sum represents the contribution of the i-th data point to the polynomial. Lagrange polynomial has many applications in various fields, in particular we have used that to help us calculate the stiffness of the cantilever provided three points in frequency vs. spring constant 2 diminsional spcae.

III. METHODS AND PROCEDURES

We worked and trained with a commercial AFM toward the beginning to end of this experiment. The AFM brand is AFMworkshop (model TT-AFM V2.2).

A. Probe and other exterior components

An essential part of AFM is the AFM probes. AFM probes are typically made of silicon and contain a sharp tip and a carrier chip. These probes interact with the sample surface to obtain the required measurements. AppNano's ACLA probes are optimized for Vibrating mode, however, they are fragile and need to be handled with care. The piezoelectric scanning stages utilize piezoelectricity to control the 3D movement of the relative tip-sample position with nanometer precision. The Piezoelectric Effect is a fundamental principle of AFM control software. A light lever is used to provide the relative vertical deflection of the cantilever by reflecting light off of the cantilever onto a position-sensitive photodetector. The piezo stages in the AFM have a lateral range of 50 μm and a vertical range of 17 μm with maximum high-voltage gain. The light lever module can be moved up and down by a coarse stepper motor (Z motor) to engage the probe with the sample. Control electronics, the micro-controller unit (MCU), and the National Instrument (NI) data acquisition device (DAQ) is contained within the Ebox. The AFM Workshop software, based on LabVIEW, controls the operation of the AFM and exports collected data. For a better understanding of the setup please refer to fig.3.

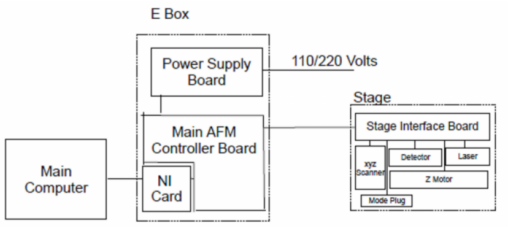

FIG. 3. The AFM and electronics diagram.[1]

Once we were ready we started by changing the probe's tip. This part could be really finicky and it requires patience and tolerance. By using the "probe exchange tool" (fig.**??**) We replaced the old probe with the new one. The key to change the probes was to gently tap the sides with the proper Angle. If it is desired to take out the probe we should face the tool downward. If it is desired to fit in a tool, we must face it upward in order to fit in the probe.

B. Softwares, Pre-scans task, and Alignments

There are 3 softwares that we need to work with. The first one is the simply a camera software were we just need for tip and region observations. The second one is the Gwyddion. Gwyddion is a free, open-source software for AFM (Atomic Force Microscopy) image processing and analysis. It allows for the visualization and manipulation of a wide range of file formats and provides various analysis tools such as roughness calculation, line profiles, and particle analysis. Additionally, it offers features like data correction, noise reduction, and filtering to enhance the quality of the image. The last which is the LabVIEW-based AFM Workshop. This software controls the AFM operation and exports collected data. It controls the motion of the sample stage, automates the tip approach, measures the resonance frequency of the cantilever for Vibrating mode, collects signals from the photodetector, and controls the feedback loop. This software is the most complicated one, and here is were all the pre-scan tasks must be done. The Pre-Scan process for the microscope involves a set of adjustments that must be made before measuring an image. The Tune Frequency window is used to select the optimal conditions for producing vibrating-mode images. The lower, selected, and upper frequencies correspond to green, blue, and red vertical bars in the oscilloscope windows. To find the resonance peak of a new probe, the lower and upper frequencies should be set to the boundaries of the probe's frequency, which is indicated on the probe box. The selected frequency should fall just to the left of the resonance peak and on the steepest part of the slope of the phase curve. The Z motor,

which raises and lowers the light lever, can be controlled manually with the speed slider or by touching the Up and Down buttons. The Automated Tip Approach button starts the process of the probe moving toward the surface, using a woodpecker motion that creates noticeable clicking sounds from the microscope stage. The Range Check option measures the usable range of the piezoelectric scanner by moving it in a square pattern that can be observed with the video optical microscope. This function must be completed before beginning a scan. Our reported value of resonance frequency is:

$f_0 = 177.56kHz$
After determining the resonance frequency, it is time to start the alignments. The experiment involves a series of three alignment procedures that include centering the sample holder, cantilever end, and camera's field-of-view, positioning the laser spot at the back of the cantilever, and aligning the reflected laser spot to the positive-sensitive photodetector's center.
Once all the proper pre-scan tasks were concluded, we started the calibration process of the AFM unit!

C. Calibration

To calibrate the Atomic Force Microscope (AFM), the calibration sample (Sample 7, AppNano Silicon Step Height Reference, Part number SHS-0.1-1) was utilized for the first scan to measure Feature B on the surface (this is just the name specified region on the sample in the manual). A topography scan of the clean area in the Feature B region of the calibration sample was performed, which covered multiple periods and included the square pits with 10 µm lateral pitch and 102 nm vertical depth (fig.4) multiple measurements of the lateral pitches along the X and Y directions, and the depths of the pits were made (we made 3 measurements). The current X/Y/Z calibration factors from the System Tab were entered into Calibration XYZ.html, along with the measured and actual values of the X/Y pitches and Z depths, and new X/Y/Z calibration factors were calculated. These newly calculated values were then input into the System Tab (A tab in the LabView software), and the changes were saved. A further topography scan was carried out to confirm the accuracy of the calibration. Once the AFM was properly calibrated, experiments were performed. With all these preliminary tasks such as alignments, calibration and probe tuning it is the time to provide our experimental procedures for the 5 experiments/activities associated with the AFM.

D. Experiment 1: Noise Floor Experiment

We performed a short experiment to measure the noise in an AFM measurement arising from both internal and environmental sources. This enables us to distinguish between actual features and noise. Additionally, we will demonstrate methods to mitigate internal and environmental noise. We conducted two topography scans with the following parameters to investigate the effects of internal and environmental noise on AFM measurements. The scans were performed in two different environments: a quiet environment with the box closed and no talking or touching the bench, and a noisy environment with the box open, talking to a partner, and light typing on the bench. Sample 8, Blank Silicon Wafer was used for the scans. The required settings for these 2 particular scans are as follows: Scan Size of 0.5 microns, Scan Rate of 1 Hz, and Scan Lines of 512. The X and Y Center should be set to (2,2),XY HV Gain to 0 and Z HV Gain of 15. We took The next set of 2 scans with the exact same conditions but setting the z HV gain to 5. Further analysis and results will be discussed on the analysis section.

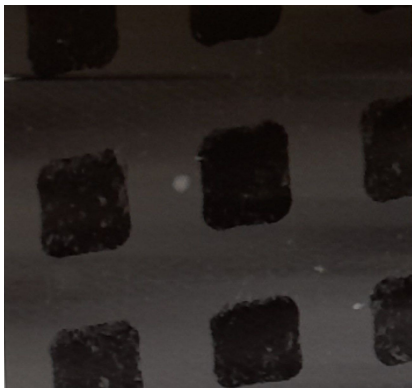

FIG. 4. A scanned profile of the calibration sample. Also note the artifacts! This is a critical skill to pinpoint the artifacts such as debris, and scratches in AFM.

E. Experiment 2: CD/DVD Experiment

In this experiment, we want to study the CD's and DVD's surface features in detail to gain a deep understanding of the working principles and capacity limitations of these optical disks. The expectation is to observe multiple holes on the surface (technical terms later in the analysis.). These holes are working as 0's and the no-hole region is actually 1. By rotation of the optical disk in a disk drive and shining a laser beam on the disk and by the principle of instructive and destructive interferences these holes will be interpreted as 0's and 1's (i.e. data). We have taken out a part of the CD and loaded that into the magnetic sample trays of the AFM. We experienced and trained on how to load and prepare a sample for atomic force microscopy in this experiment. By selecting No Background in the Display window to avoid artifacts from line leveling, we have done two scans: one from a CD, and the other from a DVD. Further analysis and results will be discussed in the analysis section.

F. Experiment 3: Hot Glue Experiment

This experiment involves the application of phase contrast to identify different materials present on a smooth surface. For this experiment, Sample 12, Hot Glue, was used. The vibrating mode was utilized with a Scan Size of less than or about 15 μm. To initiate the scanning, a clean area on the sample was selected, with the left image configured to Z DRIVE and the right image set to Z PHASE. We navigated across the sample to locate a region that has a smooth texture and good phase contrast.

G. Experiment 4: Force-Distance Curve Experiment

In atomic force microscopy, Force-Distance (F-D) curves are obtained by measuring the deflection of a cantilever as the sample is approached or moved away from the tip without active feedback. The shape of the curve depends on the length and stiffness of the cantilever, the thickness of the surface contamination layer, and the hardness of the sample. F-D curves can also convert raw T-B photodetector output to cantilever deflection and subsequently to force measurements in nano Newtons. These curves provide valuable information on the mechanical properties of the sample, such as its elasticity and adhesion, and enable researchers to analyze the interactions between the probe and the sample surface, as well as its topography.

We have used a blank silicon wafer for this experiment. The tip Approach in Non-Vibrating mode has been performed in a clean area, with a re-centering. Next, in the Force-Distance tab, the Reverse Trigger is set to T-B Signal with a value a few hundred millivolts higher than the current set point, and the Vertical Axis is set to T-B because the proportionality constant between T-B and cantilever deflection or the cantilever spring constant is unknown. The fast Rate is tested first and then Slow Rate is used for final data collection. Multiple curves are taken. To check one of our obtained data, please refer to 5. Once we have the proper analysis and conversions we can convert our plots deflection vs. z_drive curve or Force vs. z_drive. The typical appearance of the plot of Force vs. z_drive is indeed of the form of the Coulomb's force. For the sake of its importance I will reemphasize here that T-B corresponds to the voltage reading on the top and bottom part of the photodetector within the atomic force microscope.

H. Experiment 5: Boltzmann's Constant Experiment

According to equation eq.1 we need just some more quantities to calculate the Boltzmann constant. What we need is the temperature near the AFM box, and the

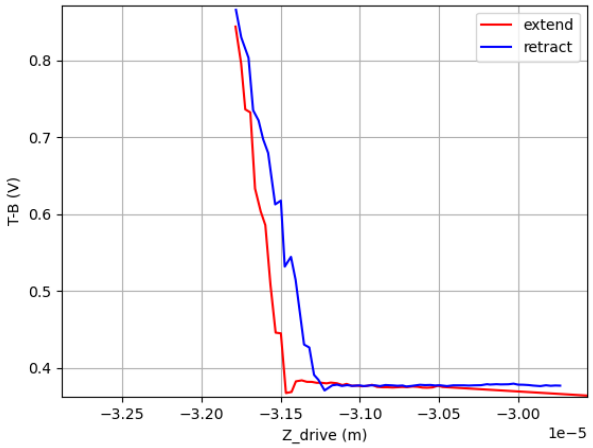

FIG. 5. The plot of T-B vs. z_drive. The Coulomb's potential pattern is clearly obvious here

$< z^2 >$. We already found the spring constant from "Experiment 4" (eq.3). The temperature is read and it was the room temperature (290 k $\pm 5k$). The next task was to find the $< z^2 >$. For this measurement, we directly accessed the raw T-B signal using the BNC cable connected to the back of the Ebox. then we connected that to a spectrum analyzer. then have the plots of power versus frequency. Note that the spectrum analyzer is picking up the thermal fluctuations of the cantilever; and we are going to exploit this to find Boltzmann constant. We imported the data to our computer for further data analysis. Note that the gain was 1 (so we did not use any pre-amplifier), and the resolution bandwidth was set to 100 Hz on the spectroscope. With these settings. The raw exported data could be seen in fig.**??**, as a plot

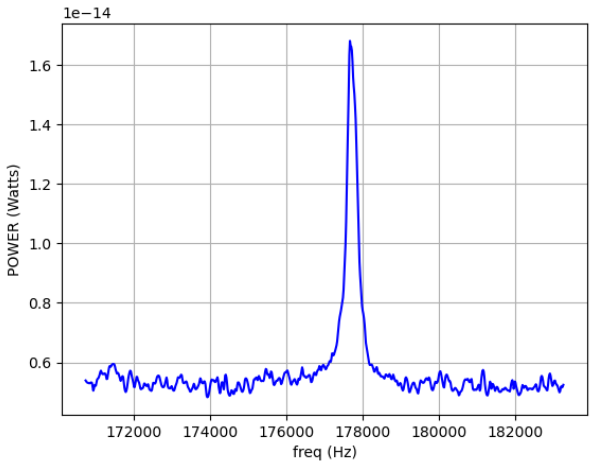

FIG. 6. Raw signal acquired from spectrum analyzer, indicating the thermal fluctuations of the cantilever.

IV. DATA ANALYSIS AND RESULTS

Here we are releasing the whole sets of data and performed analysis done on those previous outlined experiments. The results of each individual experiment are outline separately on each section.

A. Experiment 1: Noise Floor Experiment

We have generated the the four scans and plot the noise spectra (1D-FFT).The results are matching with the expectations. what we can see here is indeed confirming the normal assumption of "Noise influence your data acquisition quality"!
By considering the results of fig.12 and fig13 it could be inferred that once the environmental noise level is high, the data will be noisy. By environmental noise we mean for example: the door of the stage being open, tapping on the table, talking to the partner and etc. Once the environmental noise is absent, the noise level reduces dramatically. The Same fact is true for the internal noise sources. In our case it was the z HV gain of 15 and 5. We can clearly see on fig12, and fig13 that as the gain reduces the the noise plays a less integral role in the scanning process.

The most common noise spectra happen in order at wave numbers (k) of 0.2, 0.75, and 1.8 nm^{-1}. So after 4 scans with different conditions, it is pretty safe to infer that the dominant noise territories are as indicated. We can see the amplitude of each dominant noise varies depending on the situation in which the scan took place in. For all these same reasons the Donald A. Glaser Physics 111 B Experimentation Laboratory's personnel took many measures to reduce these noise effects. Some examples are but are not limited to designing a container and a door to contain the microscope in, setting the station at an isolated location where a minimum of interaction happens there, and designing and implementing an anti-vibration table (optical table). Shout out to our lab personnel for their insight and all their hard work.
Besides these measures, we, as scan operators, can also minimize the environmental noise by trying to at least not talk loudly and hitting the bench regularly. We should stay away from the table for the duration of the scan to get the best scan result!

B. Experiment 2: CD and DVD Experiment

Optical storage technologies have revolutionized the way digital data is stored and retrieved. Among these, CDs (compact discs) and DVDs (digital versatile discs) have gained widespread popularity due to their high storage capacity, portability, and durability. In this discussion, we will delve into the fundamental principles of how information is stored on a CD and a DVD, and the key differences between the two technologies.

CDs and DVDs store digital information in the form of tiny pits and lands on the surface of a poly-carbonate substrate. These pits and lands represent binary data, with a pit representing a 0 and a land representing a 1. When a laser beam is directed onto the disc, it is reflected off the surface of the disc, and the pattern of reflected light is used to read the binary data.

To achieve a high-quality reading of the binary data, the wavelength of the laser beam plays a critical role. For CDs, the laser beam has a wavelength of 780 nm, which lies in the infrared range of the electromagnetic spectrum. This wavelength was chosen because it balances diffraction and scattering effects, which can interfere with the reading process. Diffraction refers to the bending of light around small objects, such as the pits and lands on the disc, while scattering refers to the way that light is reflected in different directions by small objects. The 780 nm wavelength minimizes these effects and provides a reliable reading of the data.

In contrast, DVDs use a smaller laser wavelength of 650 nm, which is in the red range of the electromagnetic spectrum. This smaller wavelength allows for smaller pits and lands to be used, which enables higher storage capacity. Additionally, DVDs use a different method of encoding the data called "dual-layering," which involves layering two sets of pits and lands on top of each other. This allows for twice the storage capacity of a single-layer disc.

In the optical disk context, constructive and destructive interference refers to the way that light waves interact with the pits and lands on the surface of a CD or DVD.When a laser beam is directed onto the surface of an optical disc, it interacts with the pits and lands, which are arranged in a pattern that represents binary data. When the laser beam hits a pit, some of the light is scattered and reflected in different directions, while some of the light is absorbed by the material surrounding the pit. Similarly, when the laser beam hits a land, it is reflected back towards the detector.

When the reflected light waves from different regions of the disc interact with each other, they can either reinforce or cancel each other out, depending on their phase. This is known as interference.

Constructive interference occurs when the peaks of the waves are aligned, resulting in a stronger signal that is detected as a 1. This happens when the reflected waves from different regions of the disc are in phase with each other.

Destructive interference occurs when the peaks of the waves are misaligned, resulting in a weaker signal that is detected as a 0. This happens when the reflected waves from different regions of the disc are out of phase with each other.

Therefore, the pattern of pits and lands on a CD or DVD is designed such that the interference between the reflected light waves results in the correct representation of the binary data. By carefully controlling the size and

spacing of the pits and lands, the reflectivity of the material, and the wavelength of the laser beam, it is possible to ensure that the data can be read accurately and reliably from the disc.

Our obtained results perfectly match all the expectations that we have from our "ideal optical disks model". As demonstrated in the acquired scans after performing automated level data mean plane subtraction and a line correction by matching the height median on both optical disk samples (CD and DVD) we can see that the result is showing the pits (holes) and lands perfectly. As it is clear you can see much more lines in the DVD scan. This simply suggests that information density is much higher on a DVD than on a CD (fig.14). To back this up, we have measured the pit depth of a CD and a DVD through Gwyddion:

$depth_{cd} = 120nm \pm 4.0nm$
$depth_{DVD} = 55nm \pm 4.0nm$

and in the CD's case we get a percent difference of about 20% from the established value ($150nm$) . This means our scan and measurements were relatively precious and accurate. But on the other hand for DVD we could not achieve the same fine result and got a percent difference of 56% from the accepted value($125nm$). Unfortunately due to lack of time and perhaps hasty actions, we could not perform a fine scan and our result came out to be a bit odd on the DVD part.

C. Experiment 3: Hot Glue Experiment

In scientific terms, phase imaging is a technique utilized in Atomic Force Microscopy (AFM) to delineate discrepancies in surface characteristics, namely elasticity, adhesion, and friction, which can result in a phase shift. This phase shift is monitored simultaneously with the acquisition of topographical images, allowing for the collection of images of both topography and material properties simultaneously. Phase imaging can distinguish areas of varying surface adhesion or hardness, and also be used to detect contaminants. Please refer to figure 15 for our scan result of the hot glue. As it is obvious the scan images are not identical at all. The reason that these differences occur is due to the phase shifts happening in the types of scans. Typically, an increase in phase in the absence of topographic features indicates that the material is relatively harder. This is because the phase shift measured in AFM is related to the energy dissipation of the cantilever tip-sample interaction. When the material is harder, the tip-sample interaction becomes more dissipative, leading to a higher phase shift. By looking at the figure 15 we can conclude that the glue has been made out of more than one polymer. As we can deduce from the phase scan, at least 4 different distinct polymers are identifiable. We have identified them in figure 7.

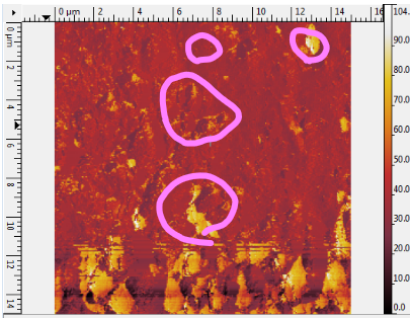

FIG. 7. As we can deduce from the phase scan, at least 4 different distinct polymers are identifiable.

D. Experiment 4: Force-Distance Curve Experiment

In this report, we present high-quality Force-Distance (F-D) curves obtained using an Atomic Force Microscope (AFM), with the vertical axis in T-B. The F-D curves show a number of distinct features, which can provide valuable insights into the mechanical properties of the sample being analyzed. One notable feature is the "snapping" behavior observed in some curves, which occurs when the tip of the AFM probe suddenly jumps into contact with the sample surface. This snapping behavior can be indicative of the presence of surface contamination or other mechanical factors affecting the probe-sample interaction. Another feature of the F-D curves is adhesion, which refers to the attractive forces between the tip and the sample surface. Adhesion can be influenced by a variety of factors, including the chemical composition of the sample and the roughness of the surface. By carefully analyzing the F-D curves, researchers can gain a more detailed understanding of the physical and mechanical properties of the sample, as well as the nature of the probe-sample interaction.

The proportionality constant between T-B signal and cantilever deflection was estimated by analyzing the F-D curves obtained from the AFM measurements. Multiple curves were taken, and their consistency was checked before averaging. The deflection sensitivity was then estimated from the slope of the linear region of the curve, which corresponds to the fairly linear regime where the cantilever behaves linearly. The slope was obtained by fitting a linear model using the Scipy library in Pyton. The corresponding uncertainty in this quantity was also found using Scipy covariance options. A plot of the curve and fitted line could be seen in fig.8. Note that the Average of the slope of the extract and retract curves were calculated and reported.

This proportionality constant turns out to be a useful piece of information for later experiments. So we call it γ from now on. Our recorded value of γ with its corresponding uncertainty is:

$$\gamma = (1470000 \pm 5900)V/m \tag{2}$$

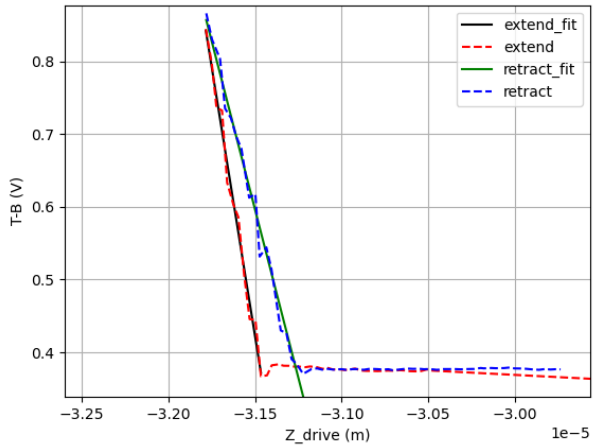

FIG. 8. The plot of T-B voltage vs, Z_drive. Fitted lines to the linear regime are shown. Note that the Average of the extract and retract's slopes were calculated and reported.

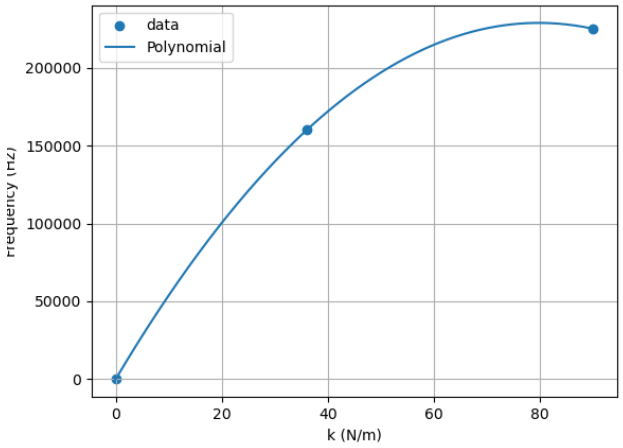

FIG. 9. The fitted Lagrangian polynomial and the three corresponding points related to the simple harmonic model.

We estimated the spring constant k of the cantilever by following a simple procedure. First, we checked the manufacturer's sheet, AppNano, for the range of resonant frequencies and spring constants of their probes. W modeled the cantilever as a simple harmonic oscillator. We then used the endpoints of the frequency and spring constant range given by the manufacturer to obtain two points along this curve. These two points were: (160000 Hz, 36 N/m) and (225000] Hz, 90 N/m). A third point was obtained using the point (0,0). Interpolating these three points with a Lagrange polynomial provided us with the exact relation predicted by the model. We also used Python's Scipy library to fit these there points on a Lagrange polynomial. To measure the resonance frequency accurately, we used the Pre-Scan tab. Finally, we plugged this resonance frequency into the polynomial equation to estimate the spring constant k of our probe. A plot of our Lagrange polynomial modeling the cantilever as a simple harmonic oscillator could be found on fig9.
Our measured value of the spring constant k with its corresponding uncertainty is:

$$k = (41.9 \pm 6.8) N/m \tag{3}$$

Now once we have the γ factor and k, the spring constant, we can simply plot the deflection vs. z_drive curve, by multiplying the vertical axis by the reciprocal of the γ .You see our deflection vs. z_drive plot on fig10.

Then After this step by multiplying the vertical axis of deflection vs. z_drive plot by k (according to Hook's law) we can obtain the Force vs. z_drive plot (fig11).

T-B is mainly due to the vertical displacement of the cantilever, as it is the most significant contribution to the cantilever deflection. But the inclination of the cantilever plays a significant role in the T-B signal. The change in the angle of the cantilever affects its stiffness, which in turn affects the deflection of the cantilever and the T-B signal.

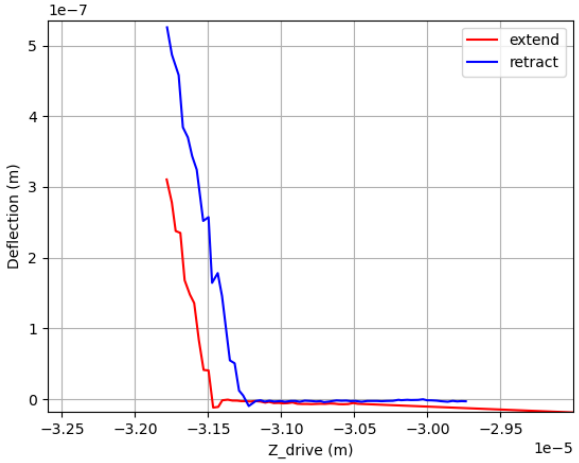

FIG. 10. Plot of the deflection vs. z_drive

Now we have every single piece of information that we need in order to complete the very last experiment!

E. Experiment 5: Boltzmann's Constant Experiment

The whole problem of calculating the Boltzmann constant will boil down to finding the $< z^2 >$. So in order to find this, we used the fig.6's data. First, we found the power per bin in this plot for each bin. Since the resolution bandwidth was 100 Hz, we ended up with multiplying the vertical axis of the plot with $\frac{1}{100}$. The quantification of the cantilever fluctuations is determined by the area beneath the peak. This is because the integration

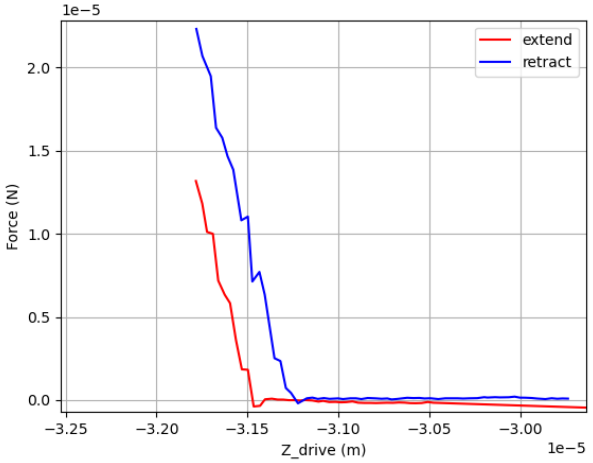

FIG. 11. The plot of the Force vs. z_drive

of the power spectrum of the fluctuations is equivalent to the mean square of the time-series data. Therefore, the estimation of the power in watts is known. Now we need to multiply this value by the internal impedance of the spectroscope (R) to get the T-B Voltage squared. Once again we have a voltage and luckily we already know the conversion of voltage to deflection. This is indeed our good old friend γ. But since this is Voltage squared, we need to multiply the final voltage by $\frac{1}{\gamma^2}$. Here you can see the summary of conversions:

$$\frac{Power}{100} * \frac{1}{\gamma^2} * (Impedance) =< z^2 > \tag{4}$$

Using this equation we can calculate our $< z^2 >$. We report that our value is:

$$< z^2 >= (9.76 * 10^{-23} \pm 0.05) m^2$$

and then using the equation 1 our estimated value of Boltzmann constant is:

$$k_B = (1.39 * 10^{-23} \pm 0.05) m^2.kg.s^{-2}.K^{-1}$$

This is remarkably a delightful result the percent difference between this value and the accepted value is certainly less than 1 percent, which is a huge accomplishment. The other measure that we could have done to make this experiment more accurate was to operate the AFM in a less crowded place where the other nose levels won't affect the thermal fluctuation of our cantilever.

V. CONCLUSION

In conclusion, our experimental work with an AFM unit has highlighted the powerful capabilities of this versatile imaging technique. Our deep understanding of the AFM microscope and the various factors that influence its functioning allowed us to successfully conduct five distinct experiments, including measuring the pit depths of optical disks, analyzing the structure of a polymer sample, and estimating the Boltzmann constant with remarkable precision. The AFM's ability to provide detailed information in all three axes of position, as well as its high sensitivity and minimal sample preparation requirements, make it a highly valuable tool for scientific research. While there are other microscopy techniques available, such as STM, TEM, SEM, and optical microscopy, AFM's ability to probe a wide range of physical and chemical properties while easily imaging nearly any sample makes it a top choice for many microscopy purposes. The only notable disadvantage of AFM is its impracticality for measuring areas greater than about 100 μm, but this is outweighed by its many benefits.

VI. REFERENCES

Inspired by AFM - Atomic Force Microscope Physics 111B: Advanced Experimentation Laboratory University of California, Berkeley [1]

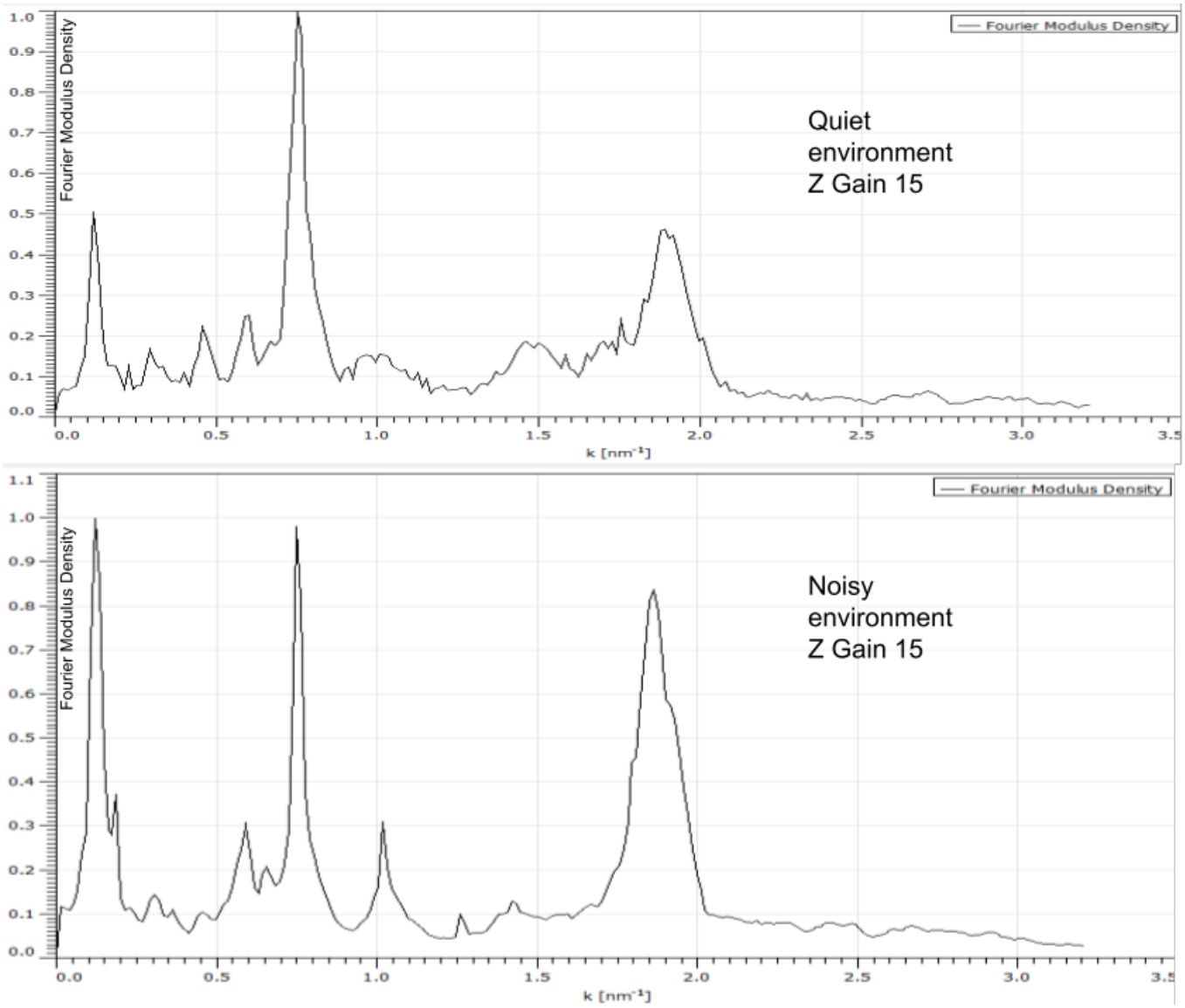

FIG. 12. Fourier transform on few lines and noise spectra for Z gain 0f 15, quiet and noisy environment series. Horizontal axis is wave number.

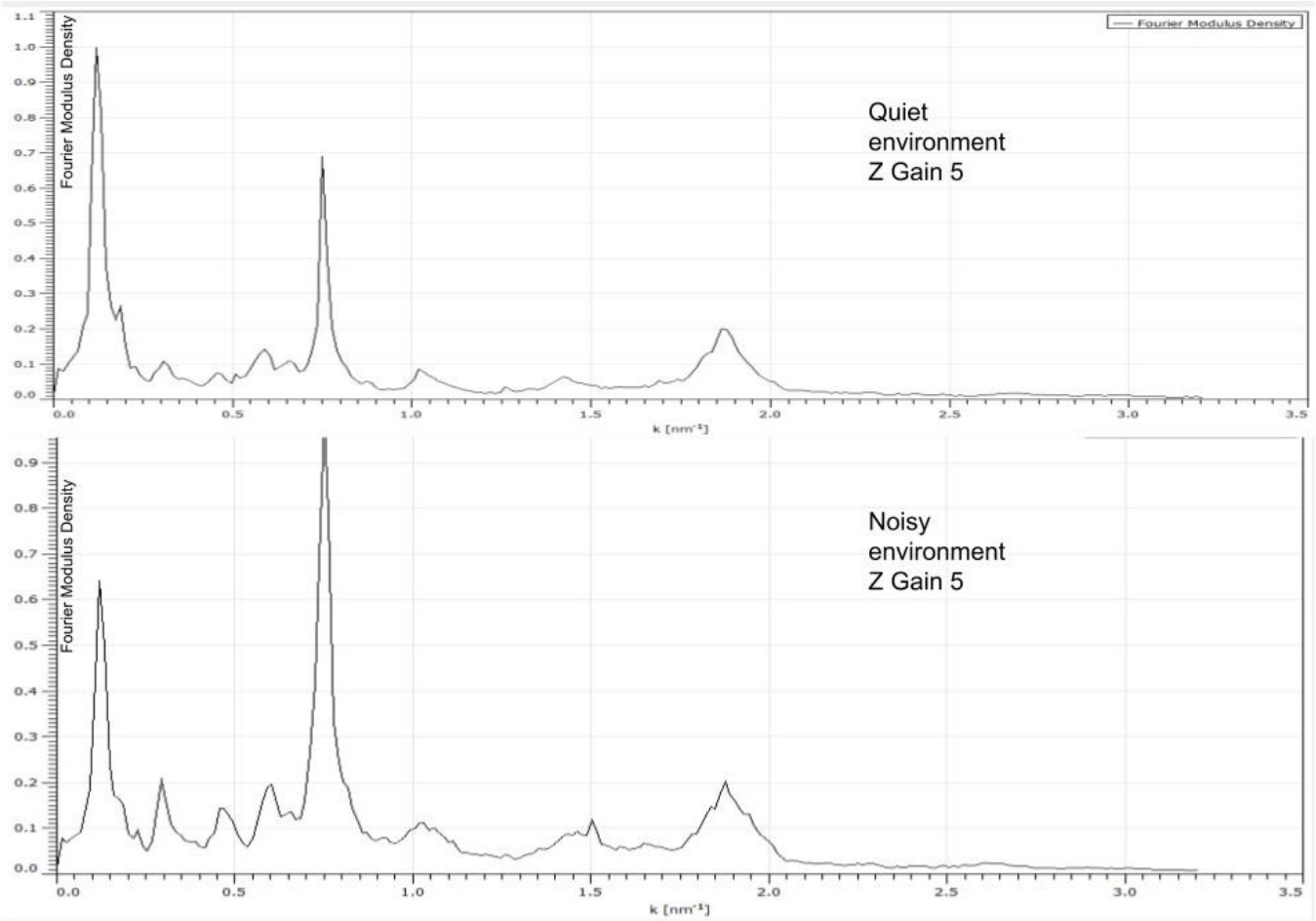

FIG. 13. Fourier transform on few lines and noise spectra for Z gain 0f 5, quiet and noisy environment series. Horizontal axis is wave number.

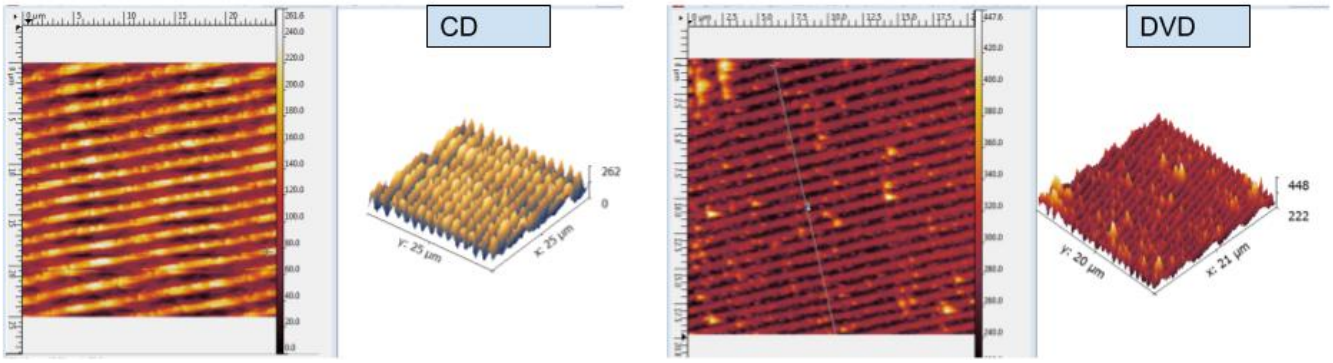

FIG. 14. The scanned image of a CD and a DVD. Note the pits and lands. Also note how the density between these two are different and hence the DVD is superior in information containment.

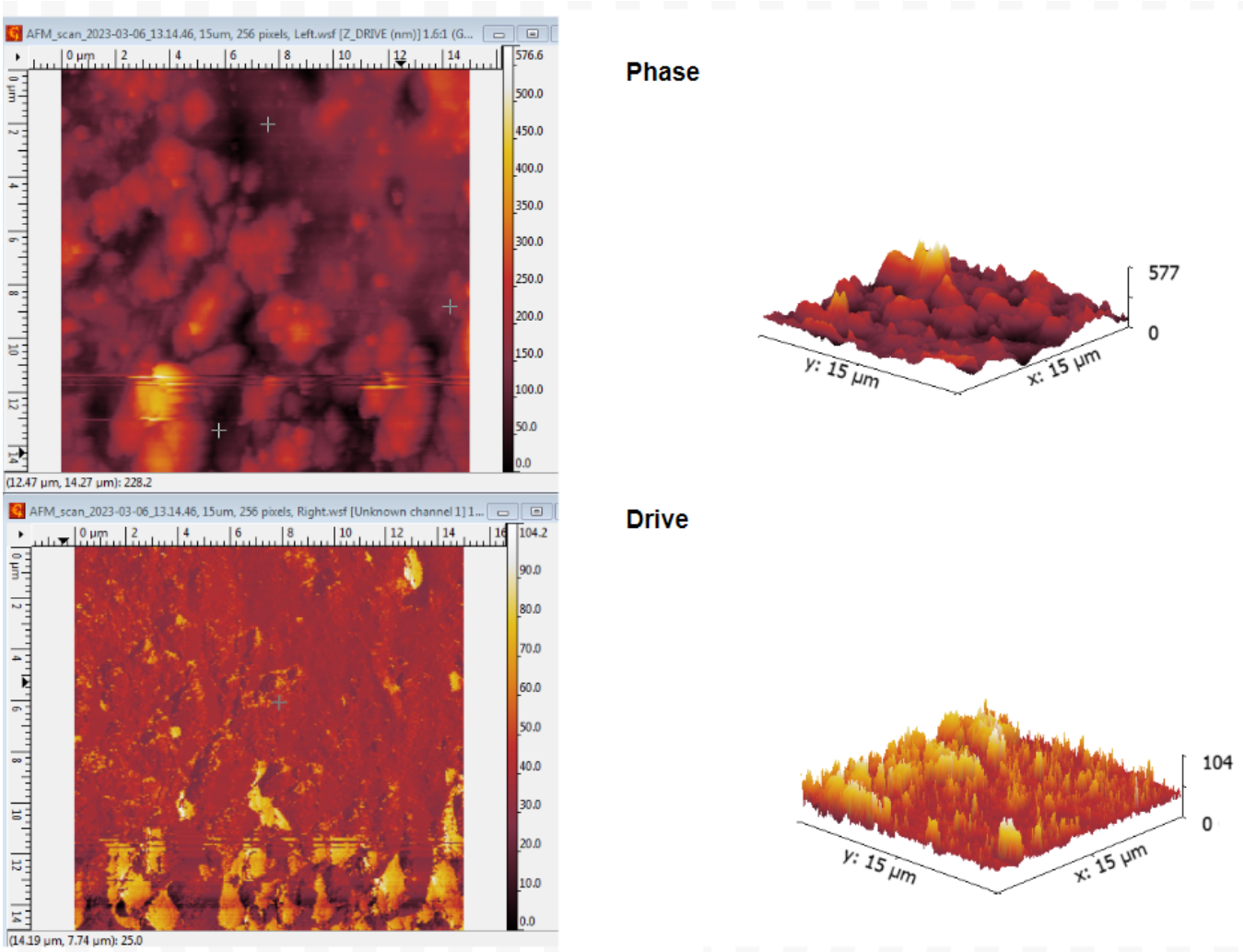

FIG. 15. The scanned images z_drive and phase of a polymer (Hot glue. Phase imaging can distinguish areas of varying surface adhesion or hardness, and also be used to detect contaminants.